Research in Pharmaceutical Sciences, October 2025; 20(5): 667-688
Received: 11-05-2024
Peer Reviewed: 30-07-2024
Revised: 05-10-2024
Accepted: 06-10-2024
Published: 20-10-2025

School of Pharmacy & Pharmaceutical Sciences
Isfahan University of Medical Sciences

*Original Article*

# Albumin conjugated with WQPDTAHHWATL and GRFLTGGTGRLLRIS peptide improves targeted docetaxel delivery for prostate cancer: an *in-silico* approach

**Karim Mahnam[1,2,*], Zeinab Karami[1], and Yaser Salehi Najafabadi[3]**

[1]*Department of Biology, Faculty of Basic Sciences, Shahrekord University, Shahrekord, I.R. Iran.*
[2]*Biotechnology Research Institute, Shahrekord University, Shahrekord, I.R. Iran.*
[3]*Cancer Research Center, Department of Internal Medicine, Hajar Hospital, Shahrekord University of Medical Sciences, Shahrekord, I.R. Iran.*

## *Abstract*

**Background and purpose:** Prostate cancer is one of the most common cancers in the world. Anti-prostate cancer drugs such as docetaxel, doxorubicin, and cabazitaxel have drawbacks resulting from their low solubility, non-targeted transfer, and many side effects. Prostate-specific membrane antigen (PSMA) receptor is expressed on the surface of prostate cancer cells. It was known that "WQPDTAHHWATL" and "GRFLTGGTGRLLRIS" peptides tended to bind this receptor.
**Theoretical approach**: "WQPDTAHHWATL" and "GRFLTGGTGRLLRIS" peptides were attached to the C and N tails of albumin protein, and an engineered albumin was designed. Then, engineered albumin and the extracellular domain of PSMA were separately simulated for 100 ns. Afterward, the interaction of engineered albumin with anti-prostate cancer drugs and the PSMA domain was investigated independently by molecular docking, molecular dynamics simulation, and molecular mechanics energies/Poisson-Boltzmann surface area binding free energy methods.
**Findings/Results:** The binding affinity order of drugs to engineered albumin was docetaxel, doxorubicin, and cabazitaxel, respectively. Also, the residence time of docetaxel was longer than that of other drugs. The final picture of complexes showed that cabazitaxel and docetaxel bound to site IB, and doxorubicin bound to site IIA of the recombinant albumin. Additionally, the C-terminus and N-terminus of the engineered albumin could bind to the PSMA receptor.
**Conclusion and implications:** It can be concluded that this engineered albumin is useful for targeted drug delivery in prostate cancer.

**Keywords:** Albumin; Molecular dynamics simulation; Prostate-specific membrane receptor; Protein docking; Residence time; Targeted drug delivery.

## INTRODUCTION

Prostate cancer is one of the most common types of cancer diagnosed worldwide, and it is responsible for approximately 30% of all cancer-related deaths globally (1).

Docetaxel ($C_{43}H_{53}NO_{14}$), cabazitaxel ($C_{45}H_{57}NO_{14}$), and doxorubicin ($C_{27}H_{29}NO_{11}$) are the main chemotherapy drugs that are used to treat prostate cancer in clinics (2,3). Docetaxel and cabazitaxel are derivatives of paclitaxel and have very similar structures and work by disrupting microtubule assembly dynamics and inducing cell cycle arrest at the G2/M phase of the cell cycle, ultimately triggering apoptosis (4). The drugs have some aromatic rings and hydrophobic properties, and they have very poor solubility, and the delivery and transfer of them in blood is difficult (2-6). The binding properties of these molecules affect the pharmacokinetic traits, such as their spreading and bioavailability (7).

*Corresponding author: K. Mahnam
Tel: +98-3832324402, Fax: +98-0384424416
Email: mahnam.karim@sku.ac.ir

| Access this article online | |
|---|---|
| | **Website:** http://rps.mui.ac.ir |
| | **DOI:** 10.4103/RPS.RPS_60_24 |

High toxicity caused by chemotherapeutic drugs and the acquisition of drug resistance by cancerous cells are the main problems in cancer therapy. For example, doxorubicin, a powerful anthracycline with a broad range of antitumor activities suitable for malignancies, has a serious restriction, where overdosing can lead to heart malfunction. In addition, toxicity is accumulative, often excluding its continued application for consequent cures involving the return of cancer (8). Therefore, targeted drug delivery is vital in medicine, especially for cancerous cells with many side effects.

One promising approach to addressing these challenges is conjugating tumor-homing peptides to drugs. These peptides can specifically target surface markers overexpressed by cancerous cells, ensuring a rapid and cancer-specific uptake of the anticancer drugs (9). The tiny peptides can also deliver selectively cytotoxic medications to malignant cells while reducing systemic toxicity to normal organs. Furthermore, they are not immunogenic and can be produced at a low cost.

Prostate-specific membrane antigen (PSMA) is a unique and specific membrane-bound glycoprotein that is overexpressed on prostate cancer cells and is also associated with the neovascularity of most solid tumors. The unique expression of PSMA makes it a vital indicator as well as a large extracellular target of imaging agents. PSMA can serve as a target for the delivery of therapeutic agents such as cytotoxins or radionuclides (10).

Tumor-homing peptides such as “GRFLTGGTGRLLRIS” and “WQPDTAHHWATL” can selectively and significantly target PSMA-expressing 22Rv1 prostate cancer cells and are the most promising prostate tumor-homing peptides (9,11).

Preparation of human serum albumin (HSA) has a low cost; it is accessible in purified form and tends to bind reversibly an enormous variety of endogenous and exogenous ligands. HSA acts as a transporter and binds to an extensive range of endogenous ligands such as fatty acids, bilirubin, thyroxine, and exogenous ligands such as penicillin, warfarin, and diazepam (12). Albumin contains 585 residues with 3 homologous α-helical domains I, II, and III. Each domain is comprised of 2 subdomains, A and B, which comprise 4 and 6 α-helices, respectively. Albumin has about 17 binding sites, including sites IA, IA/IB, IA/IIA, IB, I/II, I/III, II/III, IIA, IIA/IIB, IIA/IIIA, IIB, IIIA, IIIA/IIIB, IIIB, and IIIB′. The residues of each site were documented in the literature (13). Additional important binding sites include the free thiol located at the Cys34 residue and Sudlow sites I and II, which bind a variety of hydrophobic drugs (12). Sudlow site I is located in subdomain IIA, and Sudlow site II is located in subdomain IIIA. Among these sites, sites IB, IIA, and IIIA are more important than the other sites (13).

In a normal human, about 14 g of albumin enters the intravascular space daily. Albumin is a highly stable molecule and soluble with a very long circulatory half-life (19 days). In addition, the circulatory half-life of albumin can be increased by glycosylation and point mutations within the albumin sequence (7). For these reasons, albumin can be used for drug delivery and the circulation half-life extension of drugs (7,12). Albumin has been shown to accumulate within the tumor environment or inflamed tissues through receptor-mediated active transport, making it a capable platform for targeted drug delivery. The hydrophobic binding pockets, conjugatable thiol residue, and surface-exposed N- and C-termini in albumin serve as useful spots for carrying various kinds of peptidyl and non-peptidyl drugs (14).

Nowadays, the use of computational methods such as molecular docking and molecular dynamics simulation (MDS) in biology is fairly common. The molecular docking method predicts the binding mode and binding affinity of a ligand or drug inside the active site or on the binding site of a target 3D structure of proteins. Molecular interactions and other physical phenomena can be studied easily *via* MDS. In this method, for a specific period, the atoms and molecules can interact, providing insight into the dynamic "development" of the system, and Newton's equations of motion for a system of interacting particles are numerically solved to determine the trajectories of atoms and molecules. The forces between the particles and their potential energies are typically calculated using molecular mechanical force fields or

interatomic potentials. The methods can reveal the dynamics of large complex molecular collections and their application to drug development (15).

The coupling of small molecules to albumin has been established by Elsadek *et al*. (16) and Kratz's studies (17), in which small molecules such as doxorubicin or methotrexate are attached to albumin in the advance of anticancer and anti-rheumatic therapeutics (7). Albumin was used for the delivery of docetaxel (18-20) and doxorubicin (21-24) by other researchers previously.

To expand the pharmacokinetic profile and physical properties of albumin, several drugs have been attached to albumin either non-covalently such as insulin detemir, glucagon-like peptide-1 (GLP-1), single chain antibody (scFv), interferons-α (IFNα)-2b, fragment antigen-binding (Fab) region, anti-epidermal growth factor receptor (anti-EGFR), interleukin-1 receptor antagonist (IL-1RA), granulocyte colony-stimulating factor 3 (G-CSF), IFNα-2, Levemir®, Victoza®, ozoralizumab, and paclitaxel or covalently such as GLP-1, exendin-4, methotrexate (MTX), aldoxorubicin, and CJC-1134. Additionally, albumin has been used for genetic fusion with certain drugs such as GLP-1, G-CSF, factor VIIa (FVIIa), scFv, IFNα-2b, and Eperzan/Tanzeum (7,25).

Albumin particles were formed by high-pressure homogenization of the protein in the presence of the cancer drug paclitaxel. The FDA and EMA approved these nanoparticles under the brand name Abraxane® (26). Also, Sharma *et al*. used recombinant HSA (rHSA) to deliver 5-fluorouracil for the treatment of colon cancer. Due to the use of surfactants in the preparation of rHSA, protein aggregation is not only prevented but also provides a stable structural framework that maintains protein bioactivity throughout the life of the rHSA (27). A drug construct design incorporating binding ligands is a simple, but graceful method used for marketable reversible binding drugs, Levemir® and Victoza® (27). Larsen *et al.* have reviewed albumin-based products with a focus on the natural biological properties and molecular interactions that can be used for the design of a next-generation drug delivery platform (25).

There was no report to make recombinant albumin (RA) and use it for the drug delivery of docetaxel, doxorubicin, and cabazitaxel. Therefore, this study aimed to design a new RA with a specific binding affinity toward prostate cancer cells for the targeted delivery of chemotherapeutic drugs such as docetaxel, doxorubicin, and cabazitaxel to increase drug delivery efficiency against cancerous cells.

## METHODS

The research design included 7 steps as follows:

1. In the first step, the 3D structure of human albumin was extracted from RCSB bank (PDB code: 1AO6) with a resolution of 2.5 Å. Then, 100 ns MDS was performed on this structure. The MDS was done using Gromacs (28) under the G43A1 force field (29). The native albumin was put in the center of a triclinic box filled with SPC216 water model, and 1 nm far from the box edges. Thirteen $Na^+$ ions were substituted for water molecules to neutralize the total charge of the system. Afterward, the systems were energy minimized using the steepest descent algorithm, followed by the conjugate gradient algorithm with a tolerance of 60 kJ $mol^{-1}$ $nm^{-1}$. After energy minimization, the systems were equilibrated at constant volume (NVT) for 500 ps and constant pressure (NPT) ensembles for 1000 ps at 100 K, in which the initial structural configuration was kept fixed (29). To end, a 100 ns MDS at 310 K with a time step of 0.001 ps was done using an isothermal coupling ensemble (NPT). All covalent bonds, including polar hydrogen atoms, were constrained by the LINCS algorithm during the final phase. To avoid the edge effects and to better describe the condition of full hydration, periodic boundary conditions were applied for the protein system. Electrostatic contacts were calculated with the use of the particle mesh Ewald (PME) technique (30), and the cut-off of electrostatic and van der Waals interactions was 1 nm. All analyses were performed during the last 30 ns of the simulation (28).

2. In the second step, the 3D structures of cabazitaxel, docetaxel, and doxorubicin were obtained from the PubChem server (https://pubchem.ncbi.nlm.nih.gov/) and minimized by HyperChem 8 software (http://www.hypercubeusa.com/). Then, they docked to the final structure of native albumin that was obtained from step 1 via Autodock 4 (31). The grid box size was set at 126 × 126 × 126, and the spacing between grid points was 0.375 Å. Grid searching was performed using a local search genetic algorithm (LGA) to locate the ligands with the lowest binding energy. Routine procedures and default parameters were used in the docking. Two hundred LGA runs (32) were performed. Then, the lowest binding energy pose for drugs was selected.

3. $A(EAAAK)_2A$ linker is a rigid α-helix-forming linker and rigid spacers that can separate fairly protein domains and reduce albumin and tumor-homing peptides (GRFLTGGTGRLLRIS and WQPDTAHHWATL) interactions. The $A(EAAAK)_nA$ (n = 2-5) linker, with an α-helical conformation, is one of the proper rigid linkers that is stabilized by the $Glu^-$-$Lys^+$ salt bridges within the segments. In this work, n was considered equal to 2 (n = 2). The longer linker may lead to bowing the peptide toward albumin, resulting in improper interactions. Experimental studies have shown that this linker inhibited fluorescent resonance energy transfer efficiency between enhanced blue fluorescent protein and enhanced green fluorescent protein. Compared to flexible linkers of the same length, this helical linker could separate functional domains more effectively (33,34). Also, H4: A(EAAAK)4A and $(H4)_2$: $[A(EAAAK)4A]_2$ were used by Amet *et al.* for transferrin-based fusion proteins, and it was shown that the fusion proteins containing a helical linker, human growth hormone-$(H4)_2$-transferrin and transferrin-$(H4)_2$-human growth hormone, were expressed 1.7- and 2.4-fold higher, respectively, with a 2-fold lower $ED_{50}$ (the dose of a fusion protein that led to half of the maximum proliferation) than the human growth hormone-transferrin fusion protein without a helical linker. The transferrin-$(H4)_2$-G-CSF fusion protein exhibited a greater expression with an 11.2-fold increase compared with the transferrin-G-CSF fusion protein (35). In addition, Bai *et al.* indicated that the insertion of $(H4)_2$ linker between G-CSF and transferrin domains in the recombinant fusion protein could significantly improve myelopoietic activity over the non-linker fusion protein (36). This linker was put between albumin and tumor-homing peptides for the inhibition of their interactions to make "full peptides" [GRFLTGGTGRLLRISA$(EAAAK)_2$A] and [A$(EAAAK)_2$AWQPDTAHHWATL] to the N-terminal and C-terminal of albumin, respectively, in step 3. In this step, because the Jpred4 server (https://www.compbio.dundee.ac.uk/jpred/) (37) predicted the structure of full peptides as a helix structure, the 3D structure of full peptides was made as a helix in HyperChem 8 software and minimized *via* the steepest decent algorithm with a root mean square (RMS) gradient of 0.1 kcal/(Å mol). Then, the C-terminal and N-terminal of the first and second full peptides, respectively, were connected to the surface-exposed N-terminal and C-terminal of the final structure of albumin that was obtained from step 1 *via* Discovery Studio software (https://www.3ds.com/products-services/biovia/) to make RA. This structure had 2 "full peptides" in its C-terminal and N-terminal, and the linkers separated tumor-homing peptides from albumin. Then, 100 ns MDS with the same previous procedure was done (step 1), and the final structure was used for step 4.

4. In step 4, docking drugs to the simulated RA was done with the same previous docking procedure (step 2), and the lowest binding pose of complexes was selected for 100 ns MDS. The topology of drugs was made by the Prodrg server (http://davapc1.bioch.dundee.ac.uk) and included in the RA protein topology.

Binding free energy is an important thermodynamic factor, providing detailed information about the ligand-protein interactions (38). The binding free energy of ligands was calculated by the molecular mechanics/Poisson-Boltzmann surface area (MM/PBSA) method from the single-trajectory method of the complexes. In this method, $\Delta G_{binding}$ is calculated from the free energies of the ligand-protein system during 100 ns MDS using the following equation:

$$\Delta G_{binding} = G_{complex} - (G_{protein} + G_{ligand})$$

where, $G_{complex}$, $G_{ligand}$, and $G_{protein}$ were considered the absolute free energy of complex, ligand, and protein, respectively. The

g_mmpbsa script was applied to compute the binding free energy of these compounds (39). More details of MM/PBSA binding free energy were explained previously (38,39). Forty-eight snapshots were taken with 2100 ps intervals for each complex structure, and binding free energies were calculated for each snapshot and averaged during the last 30 ns of MDS (29).

5. In step 5, the 3D structure of the extracellular domain of the PSMA membrane protein (chain A) was extracted from the RCSB bank (PDB code: 1Z8L) and simulated for 100 ns. Because the RA protein has to bind only to the extracellular domain of the PSMA protein, and intramembrane or intracellular parts of it were not necessary, the other chains of PSMA were omitted in this study. The final structure was used for the next step.

6. In this step, the simulated PSMA was docked to the C- and N-termini of RA separately *via* the Haddock server (https://wenmr.science.uu.nl) (40), and the PSMA-RA complexes were obtained. In the recent study, it was mentioned that Lys207, Phe209, Tyr234, Gln254, Arg463, Asp465, Arg511, and Tyr700 of the PSMA receptor were bonded to the "WQPDTAHHWATL" peptide (11). Then, these residues of the PSMA protein and the C-terminal or N-terminal tails of RA (WQPDTAHHWATL or GRFLTGGTGRLLRIS peptides) were considered active residues for the Haddock server. The best haddock score structures were used for the next step as PSMA-RA complexes.

7. In step 7, the obtained 2 PSMA-RA complexes were simulated for 100 ns separately with the same previous MDS conditions, and the analyses were performed during the last 30 ns of MDS.

### *Residence time of drugs at the binding site*

Calculating the dissociation rate constant or residence time was more difficult than calculating the binding affinity. Unlike the binding affinity, which could be determined using the two-state endpoint method, calculating dissociation rates required a large sample of the transition state, which could occur in more than one pathway in the protein-ligand configuration space. Since the residence time of interesting therapeutic compounds (minutes to hours) was beyond the time available for conventional molecular stimulation. It was suggested that the residence time estimated directly from some enhanced MDS (41).

This study used random acceleration molecular dynamics (RAMD) to calculate the residence time of drugs (41). It was based on the random force in the MDS method, an advanced modelling technique originally developed to investigate exit pathways from binding sites of proteins (42). In the RAMD method, during MDS of the complex, a small additional randomly oriented force was applied to the ligand to facilitate easy unbinding. Simulations were stopped when the center of mass of the ligand had moved further than 4 nm from its original position (ramd-max-dist) (41). Thus, this method allowed observing the evolution of the ligand in a short simulation time of a few picoseconds or nanoseconds. The size of the random force was 585 kJ $mol^{-1}nm^{-1}$ in this work and equal in all simulations; then, it did not affect the computed relative residence times (41).

For each complex, 21 structures ("gro" files) were extracted from the last 5 ns of the 100 ns MDS trajectory with a time interval of 250 ps, and 21 RAMD simulations were performed for each structure. Then, the atomic coordinates and velocities used for RAMD simulations were different. Then, the simulation of dissociation trajectories or residence time for each starting replica (21 structures) was estimated and averaged. In total, 63 RMAD simulations were done for 3 complexes.

### *Statistical analysis*

The statistical analysis was performed with the IBM SPSS Statistics 27 software package. Data were expressed as mean ± standard deviation. A parametric test of one-way ANOVA analysis was used to compare the means of the parameters. The $P$-value < 0.01 was considered statistically significant.

### *Supplementary materials*

The supplementary materials for this article can be found online at: https://www.dropbox.com/scl/fi/mjowei02hjyfpk42fmtw9/Supplementary-RPS-60-24.pdf?rlkey=oe6wnburkb8z3cl2qmquh64zk&st=qjxuz9tn&dl=0

## RESULTS

### *Docking and MDS drugs to native and RA*

The average backbone root mean square deviation (RMSD) of native albumin (without "full peptide") in step 1 during the last 30 ns of MDS was 0.36 ± 0.01 nm. The backbone RMSD plot of native albumin is presented in Fig. S1. Then, the native albumin structure reached equilibrium after about 70 ns MDS. The final structure of unmodified albumin (without "full peptides") and RA (albumin with "full peptides") after 100 ns MDS was used for docking studies. The best binding free energy (the lowest binding free energy) of cabazitaxel, docetaxel, and doxorubicin to unmodified albumin (step 2) was -3.19, -5.29, and -6.46 kcal/mol, and the binding free energy of these drugs to RA (step 4) was -5.76, -5.96, and -8.57 kcal/mol, respectively.

Because docetaxel and cabazitaxel had similar structures, and both of them were derivatives of paclitaxel, their best docking energies were alike, especially in RA. The negative binding free energies showed that these drugs could bind to both unmodified albumin and RA. The negative potential in MDS steps, or steps 1, 3, and 4, of all systems showed that all systems were stable. The average temperature during the last 30 ns of MDS was about 310 K with a trivial standard deviation, revealing that all systems reached temperature equilibration. Figure 1 represents the backbone RMSD in RA either without drug (step 3) or in complex with drug (step 4), as well as the backbone RMSD in drugs without RA (step 4) during 100 ns MDS.

The high backbone RMSD of free RA was probably due to the high fluctuation of "full peptides" at RA tails, but finally, during the last 30 MDS, the standard deviation of the backbone RMSD became small (0.02 nm), and the free RA reached a stable structure. The small standard deviation of the backbone RMSD of RA in complex with drugs during the 30 ns MDS indicated that all systems reached structural equilibration after about 70 ns, and the simulation time was enough. Then, all analyses were performed during the last 30 ns of MDS. As revealed in Fig. 1, the backbone RMSD of RA decreased after binding to drugs relative to free RA. The cause of this event is probably that the starting structure for complexes was obtained from a free RA simulation, or the hydrogen and hydrophobic interactions between drugs and RA led to a decrease in RMSD of RA in complexes. Also, a trivial standard deviation of RMSD of drugs in complex with RA showed that drugs reached equilibrium and did not change their positions relative to initial docking positions, especially during the last 30 ns of MDS, because they had proper interactions with RA. It means docking has found proper sites for drugs (Fig. 1).

Table 1 shows the average of the backbone RMSD, radius of gyration (Rg) of RA, the average of the backbone root mean square fluctuation (RMSF), the average accessible surface area (SASA), th e average number of contacts (ANC) between drugs and RA, and the average number of hydrogen bonds (ANHB) between drugs and RA during the last 30 ns of 100 ns MDS in the simulation of free RA and RA in complexes (steps 3 and 4).

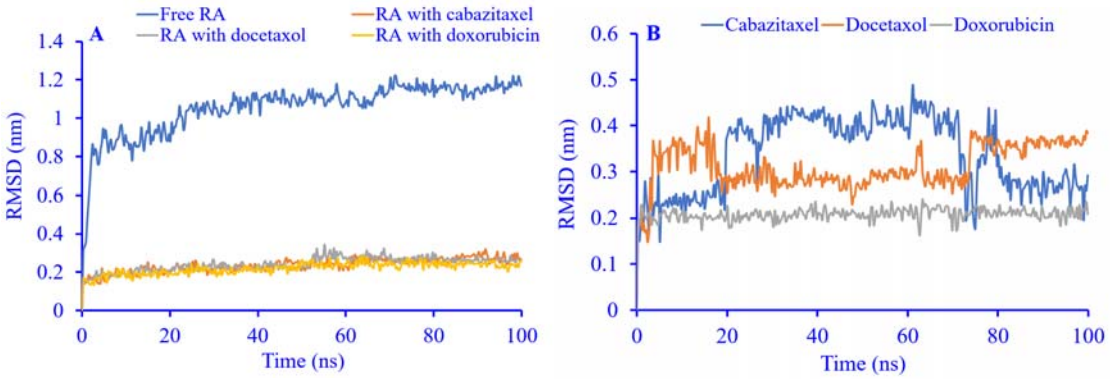


**Fig. 1**. The backbone RMSD of (A) RA without drugs (free RA) and in complex with drugs and (B) RMSD of drugs during 100 ns simulation. RA, Recombinant albumin; RMSD, root mean square deviation.

**Table 1.** The simulation results of RA in complex with drugs during the last 30 ns of the 100 ns simulation. Data were expressed as mean ± standard deviation.

| | Backbone RMSD of RA (nm) | Backbone RMSF (nm) | Rg (nm) | RMSD of drugs (nm) | SASA of RA ($nm^2$) | ANHB of RA with drugs | ANC of RA with drugs | ANHB of RA with itself |
|---|---|---|---|---|---|---|---|---|
| **Free RA** | 1.15 ± 0.02 | 0.11 ± 0.05 | 2.66 ± 0.01 | - | 273.5 ± 3.5 | - | - | 514.3 ± 11.9 |
| **RA-cabazitaxel** | 0.26 ± 0.01 | 0.11 ± 0.05 | 2.67 ± 0.01 | 0.28 ± 0.05 | 277.8 ± 3.2 | 0.15 ± 0.39 | 54.54 ± 7.09 | 508.3 ± 10.8 |
| **RA-docetaxel** | 0.26 ± 0.01 | 0.11 ± 0.04 | 2.63 ± 0.008 | 0.35 ± 0.02 | 272.4 ± 3.5 | 0.81 ± 0.78 | 67.78 ± 1.35 | 509.9 ± 12.8 |
| **RA-doxorubicin** | 0.24 ± 0.01 | 0.09 ± 0.03 | 2.67 ± 0.01 | 0.21 ± 0.01 | 275.4 ± 3.2 | 1.55 ± 1.05 | 50 | 509.4 ± 11.3 |

RA, Recombinant albumin; RMSD, root mean square deviation; RMSF, root mean square fluctuation; Rg, radius of gyration; SASA, solvent accessible surface area; ANHB, average of hydrogen bonds number; ANC, average number of contacts.

The small standard deviation of the Rg confirmed that all systems reached equilibrium and had stable structures after about 70 ns of MDS. Also, the Rg of free RA (step 3) was almost the same as RA in complexes (step 4), which means binding drugs did not change the compactness or the tertiary structure of RA. The SASA analysis was used to measure the degree to which residues of a protein were exposed to their environment. The total SASA of RA, despite our expectations, was almost constant after binding drugs to RA. The cause of this event is that binding drugs to RA probably leads to more exposure to the C-terminal and N-terminal of RA or other parts of RA, and this neutralizes the decrease of the accessible surface area of RA arising from binding drugs to RA (Table 1).

The average of the backbone RMSF in free RA and RA in complex with drugs was almost constant, which means binding drugs did not change the total flexibility of RA residues. Also, a comparison of RMSF of RA residues that were in contact with drugs relative to the same residues in free RA showed that the RMSF or flexibility of these residues did not change (Table 1).

The average number of hydrogen bonds of RA with itself decreased after binding drugs to it. The case of this event was that after binding drugs to RA, some atoms of the RA interacted with drugs and could not interact with other protein atoms, and then the number of hydrogen bonds of RA with itself decreased. All drugs made hydrogen bonds with RA. The highest average of the number of hydrogen bonds between drugs and RA belonged to doxorubicin, docetaxel, and cabazitaxel, respectively. Of course, hydrophobic interaction was more important than hydrogen bonds in the interaction of drugs with RA (Table 1).

The ANC (distance less than 6 Å (43)) between drugs and RA belonged to docetaxel, cabazitaxel, and doxorubicin, respectively (Table 1).

Also, the visual inspection of the final structure of RA revealed that albumin and tumor-homing peptides had no inappropriate interactions, and the length of the linker was suitable. Also, the secondary structure of free RA and in complex with drugs was calculated *via* the "gmx do_dssp" module of the Gromacs package and revealed a few decreases in the α-helix content of RA upon drug binding (63.8%, 62.1%, 62.4%, and 62.3% for free RA, RA-cabazitaxel, RA-docetaxel, and RA-doxorubicin, respectively) (Table 1).

### *Principal component analysis*

It is well established that protein atom dynamics have vital roles in the folding, structural stability, flexibility, and function of proteins (44). The potential energy surface of proteins or the phase space of proteins is very complex and huge, and shows the probability of the existence of a protein conformation in each specific bond length, angle, and torsion angle. Because thousands of bond lengths and angles exist in a protein, drawing a thousand-dimensional plot for a protein is impossible. Principal component analysis (PCA), or analysis of elementary components, is a mathematical technique based on a covariant

matrix of Cα displacement of protein. Principal components (PCs) were obtained by diagonalizing the covariance matrix of Cα displacement and named eigenvectors. The eigenvectors are directions in conformational space and represent the collective motions of atoms along those directions. The eigenvalues represent the mean square fluctuations of atoms along corresponding eigenvectors (44). By using this method, we could determine the original vectors of movement of a protein in the space phase (45) and also prepare useful information for ligand binding (44). It has been shown that the most internal motion of a protein is confined within a subspace of very small dimensions (45). Then, only the first 2 PCs with the highest eigenvalues were considered in this study. The "gmx covar" command was used for PCA analysis in this study, and the projections of trajectories onto the eigenvectors were accomplished *via* the "gmx anaeig" module of the GROMACS package (44). It has been revealed that the first 2 PCs can correctly describe the folding or unfolding pathways (45). PCA analysis can be performed on the high-dimensional phase space of protein molecular motions and reduces data noise. PCA can also visualize the dimensionally rich phase space and can detect transitional states in protein folding and probable conformational changes due to drug binding (45).

In this study, the first 2 eigenvectors of principal components (PC1 and PC2) that had the most eigenvalues on the trajectory file of complexes were used for PCA analysis. The first 2 eigenvalues for free RA were 1.73 and 1.43. These values for RA in complex with cabazitaxel, docetaxel, and doxorubicin were 3.91 and 1.89, 4.4 and 2.43, and 3.35 and 1.15, respectively. Also, this study found that the first eigenvectors were almost two-fold as important as the second eigenvectors.

At first, the diagram of PC1 versus PC2 of Cα displacement during the last 30 ns of MDS for free RA and in complex with drugs obtained (Fig. S2). As shown in Fig. S2, the bindings of drugs to RA induced different changes in the Cα main displacement of the RA structural movements.

Free energy landscape (FEL) represents a perception of how proteins fold. FEL is made based on PC1 and PC2 and structural changes in protein complexes. In this method, free energy, or G(PC1, PC2) of protein is calculated by $-k_BTlogP(PC1, PC2)$, in which $k_B$ is the Boltzmann constant, T is the absolute temperature, and P(PC1, PC2) is the probability density function of the existence of a conformation in a specific PC1 and PC2.

Lately, the energy landscape model, which was initially used to study protein folding problems, has been extended to study ligand-protein binding (46,47). Therefore, the FEL of free RA or in complex with drugs versus PC1 and PC2 was calculated during the last 30 ns of MDS using the "gmx sham" command (44), which was represented in Fig. 2. As shown in Fig. 2, the red pecks showed the high-energy regions or thermodynamically unstable states, or transition states between stable states (wide blue basins) in the phase space of RA in free or complex form. In the vast basin blue regions, the free energy was low, and they were probable states. Because the blue regions in the free and complex forms were wide, it can be concluded that simulations were converged, and RA obtained many stable conformations and low energy conformations during the last 30 ns of MDS. As revealed in the FEL diagram of RA, the wide basin areas corresponded to the vast stable states observed in the RMSD plot, especially in the last 30 ns of MDS. Also, FEL was a few different in all complexes and free RA, which means all drugs bound to RA, and binding each drug produced a different main displacement in protein Cα movement in protein structure. Also, the range of free energies in complexes (about 0.01 kJ/mol) was less relative to free RA (about 0.05 kJ/mol), which means binding of drugs to RA leads to less unstable conformations or more stable conformations. The presence of drugs modified the displacement in protein Cα movement of RA, which corresponded to an induced fit model of protein-ligand binding and population shift. Luckily, these conformational changes were small and not very high. High conformational change in albumin can lead to more clearance from the blood through the gp18/gp30 system and a reduction in circulatory half-life (7).

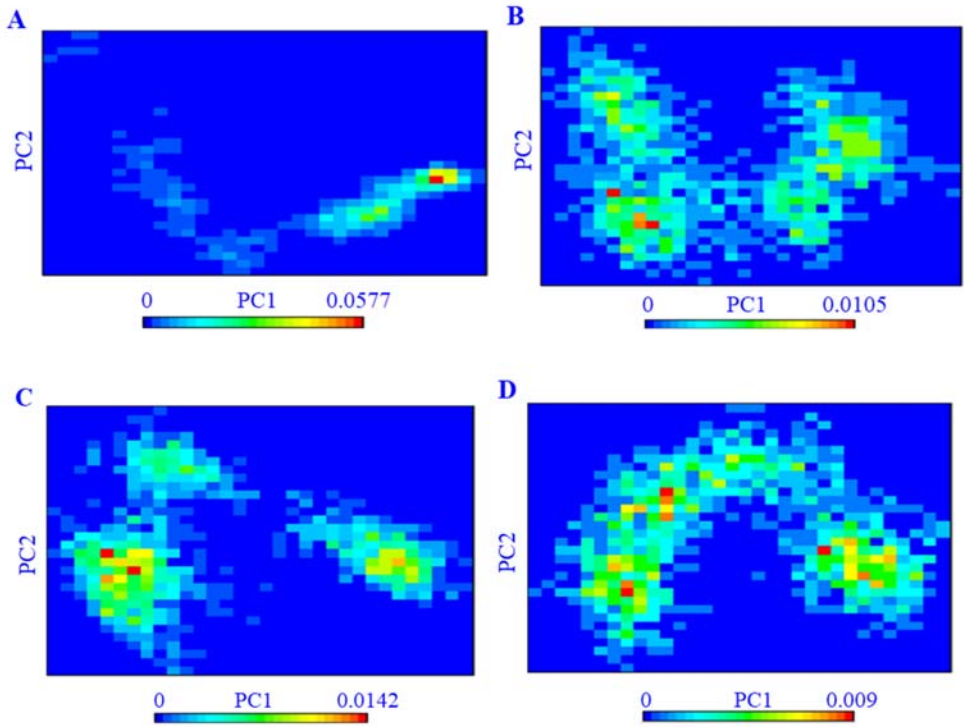


**Fig. 2.** The free energy landscape of free and bonded RA during the last 30 ns of simulation. (A) Free RA; (B) complex RA with cabazitaxel; (C) complex RA with docetaxel; (D) complex RA with doxorubicin. RA, Recombinant albumin.

Figure 3 shows the 2D and 3D interactions of drugs at the end of 100 ns of MDS in the complexes of RA. The binding residues were revealed *via* LigPlot software (https://www.ebi.ac.uk/thornton-srv/software/LigPlot/) (48). According to Fig. 3, in the complex of RA with cabazitaxel, 14 residues, including Arg81, Glu82, Thr83, Tyr84, Gly85, Asp108, Asn109, Pro110, Arg145, Ser419, Lys466, Thr467, Val498, and Lys534 of RA, had interactions with cabazitaxel. These residues mostly belonged to site IB. It can be concluded that cabazitaxel binds to site IB of RA. In the final structure of complex docetaxel, 18 residues, including Phe36, Arg114, Leu115, Val116, Pro118, Met123, Ala126, Phe127, Phe134, Lys137, Tyr138, Tyr140, Glu141, Ile142, Tyr161, Phe165, Leu182, and Arg186, had hydrophobic and electrostatic interactions with this drug. Then, generally, residues 114-186 act as docetaxel binding domains in RA. Almost all these residues belonged to site IB or were very near this site. In complex doxorubicin, 22 residues, including Glu153, Lys195, Lys199, Trp214, Arg218, Gln221, Arg222, Glu294, Asn295, Pro339, Asp340, Tyr341, Val343, Val433, Lys436, Cys437, His440, Lys444, Pro447, Cys448, Asp451, and Tyr452, had hydrophobic and electrostatic interactions with this drug (Fig. 3). Most of these residues belonged to site IIA, and they were hydrophobic, which was rational because of the hydrophobic nature of doxorubicin. Overall, these results revealed the binding of drugs to RA qualitatively. Then, to determine the binding affinity of drugs to RA quantitatively, a MM/PBSA binding free energy calculation was performed at the end of step 4.

### *MM/PBSA binding free energy*

The MM/PBSA binding free energies of drugs to RA during the 100 ns MDS were calculated *via* the g_mmpbsa script (38,39) and represented in Fig. 4, and the averages during the last 30 ns of MDS were indicated in Table 2.

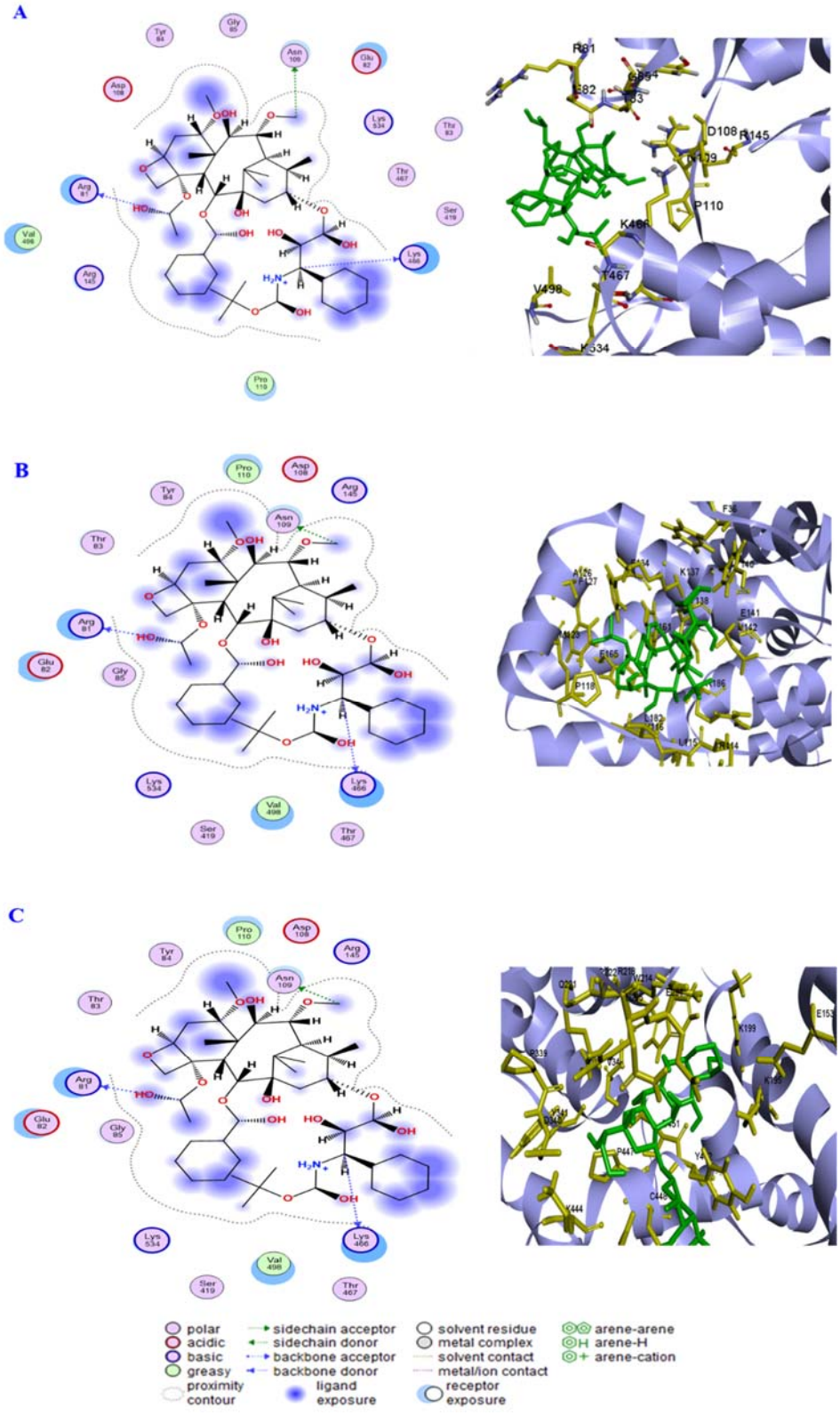


**Fig. 3.** The 2D and 3D interactions in final pictures of drugs in the binding site of recombinant albumin after 100 ns simulation. (A) Cabazitaxel; (B) docetaxel; (C) doxorubicin. The drugs were coloured in green.

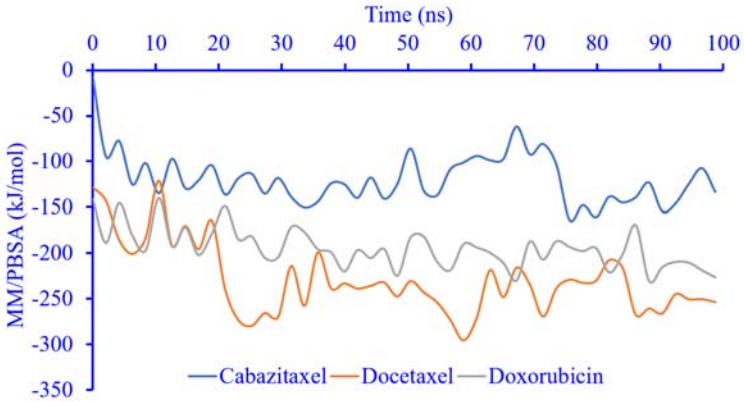


**Fig. 4.** The molecular mechanics energies/Poisson-Boltzmann surface area (mm/pbsa) binding free energies of drugs to recombinant albumin during the 100 ns simulation.

**Table 2.** The average of MM/PBSA binding free energies and the sum of VDW interactions and non-polar solvation and also the sum of electrostatics interactions and polar solvation energies (kJ/mol) of drugs to recombinant albumin during the last 30 ns of simulation. Data were expressed as mean ± standard deviation.

| | MM/PBSA binding energy | Sum of VDW interaction and non-polar solvation | Sum of electrostatic interaction and polar solvation |
|---|---|---|---|
| **Docetaxel** | -244.1 ± 19.3 | -310.46 | 66.35 |
| **Doxorubicin** | -205.7 ± 16.5 | -286.86 | 81.12 |
| **Cabazitaxel** | -133.6 ± 23.5 | -177.64 | 43.99 |

MM/PBSA, molecular mechanics/Poisson-Boltzmann surface area; VDW, Van der Waals.

Also, one-way ANOVA analysis showed that all differences in means of binding energies were significantly different, and all *P*-values between the means of energy of each pair of drug binding energies were less than 0.01. These results showed that all drugs had negative binding free energy to RA during 100 ns MDS, and then the RA could be used for the delivery of drugs. According to MM/PBSA binding free energy, the order of binding affinity for drugs was docetaxel > doxorubicin > cabazitaxel. Also, the sum of van der Waals (VDW) interactions and non-polar solvation contributions in binding drugs was more negative and more important than the sum of electrostatic interactions and polar solvation energies. The essence of binding, as seen in docking results, was hydrophobic interaction due to the existence of the aromatic rings in drug structures. As mentioned before, the order of binding affinity of drugs to RA in docking was doxorubicin > docetaxel > cabazitaxel. In both methods, cabazitaxel had the least binding affinity, but in the MM/PBSA binding free energy method, docetaxel, and in the docking method, doxorubicin had better interaction with RA. The cause of this difference is that the results of docking are raw and static and obtained from the rigid binding site without considering water molecules explicitly, and they are not as precise as MM/PBSA binding free energy results that were obtained during the dynamics and flexible interactions of drugs with the binding sites in explicit water molecules conditions. The docking results are usually used for virtual screening and obtaining the initial complex structure for MDS.

According to MM/PBSA results, the main contributor residues of RA with binding free energy less than -3 kJ/mol with drugs during the last 30 ns consisted of Glu82, Glu465, Thr467, Pro468, Val498, and Pro499 in the cabazitaxel complex, and Arg117, Pro118, Val122, Met123, Phe134, Lys136, Lys137, Tyr138, Arg144, Arg145, Phe165, and Leu182 in the docetaxel complex, and finally, Trp214, Val343, Lys439, His440, Lys444, Arg445, Pro447, Cys448, Tyr452, and Val455 in the doxorubicin complex. These residues were identical to or near those residues that were obtained from the final snapshot in the MDS of complexes. Although, there were the trivial differences because the contributor residue belonged to the dynamic picture of interactions

during the last 30 ns MDS and was related to only some residues that had binding free energy less than -3 kJ/mol, but the residues in Fig. 3 were related to the final static snapshot of all contributor residues in complexes. Overall, it can be concluded that proper binding of drugs with RA could occur, and this engineered protein could be used for transferring these anticancer drugs. The binding residues were similar to binding residues obtained from docking (step 2). In total, the simulation results and docking results were compatible.

### *Residence time*

The residence time was defined as the simulation time required for ligand dissociation in 50% of the trajectories. At first, 21 residence times for each drug were obtained from RAMD simulations of complexes. Then, a quantile-quantile (QQ) plot (49) of the residence times of drugs was drawn and indicated in Fig. S3. Because the points on the QQ plot fell on the 45-degree reference line, the residence times of all drugs to RA had almost normal distributions. Then, we could do parametric statistical analysis, such as one-way ANOVA.

Subsequently, the outlier time was omitted for each drug, and the time required for dissociation of 50% of trajectories was calculated, which was 135, 63, and 49 ps for docetaxel, cabazitaxel, and doxorubicin, respectively. One-way ANOVA analysis showed that the *P*-values between means of the residence time of all pairs of drugs were zero except for the cabazitaxel and doxorubicin pair ($P$ = 0.189). It means the residence time of cabazitaxel and doxorubicin was almost equal and did not significantly differ in the 95% confidence interval. On the other hand, the residence time of 2 drugs was less than that of docetaxel and was significantly different from it. Also, the average residence time after the omission of outliers was 135.9 ± 41.3, 67.2 ± 25.3, and 49.3 ± 12.8 ps for docetaxel, cabazitaxel, and doxorubicin, respectively. If we consider the standard deviations of the values for cabazitaxel and doxorubicin, the similarity between them is confirmed in one-way ANOVA analysis.

The ranking order of these times was the same as the number of contacts between drugs and RA. Then, we could conclude that residence time had a direct relationship with the number of contacts between protein and ligand. The results of the MM/PBSA binding energy method showed proper interaction of docetaxel with RA that was compatible with a longer residence time of this drug relative to other drugs. Then, the kinetics and thermodynamics results were well-matched. In total, the results of residence time showed that the drugs could dissociate from RA during some picoseconds. Then, RA could release drugs into cancer cells.

### *MDS and docking results related to the PSMA receptor*

After binding drugs to RA, this protein should bind to the extracellular domain of the PSMA receptor on the cancerous cell surface. Then, docking and MDS of RA with the extracellular domain of the PSMA receptor were investigated. Figure 5 shows the backbone RMSD of the free extracellular domain of the PSMA receptor during 100 ns of MDS (step 5).

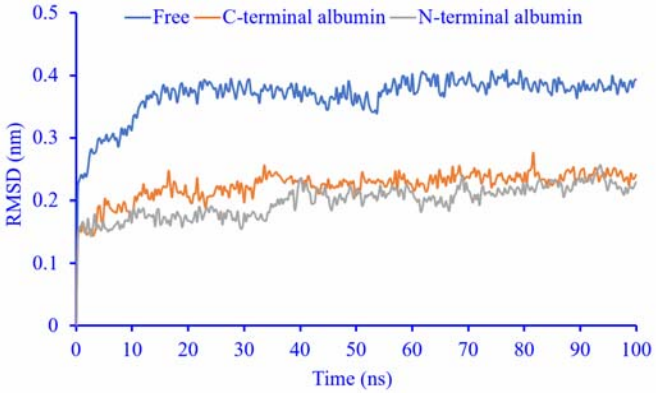


**Fig. 5**. The backbone RMSD of free prostate-specific membrane antigen domain receptor and in complex with the C-terminal and N-terminal of recombinant albumin. RMSD, Root mean square deviation.

**Table 3.** The average simulation results for the free PSMA receptor and PSMA receptor in complex with the C-terminal and N-terminal of RA during the last 30 ns of simulation. Data were expressed as mean ± standard deviation.

| | RMSD of PSMA in complex (nm) | Rg of PSMA (nm) | ANHB between RA and PSMA | Rg of RA in complex (nm) | Backbone RMSF (nm) | SASA of PSMA ($nm^2$) | ANC of RA with PSMA | SASA of RA ($nm^2$) |
|---|---|---|---|---|---|---|---|---|
| **Free PSMA** | 0.38 ± 0.008 | 2.48 ± 0.006 | - | - | 0.09 ± 0.04 | 255.32 ± 3.43 | - | - |
| **PSMA in complex with C-terminal RA** | 0.23 ± 0.008 | 2.49 ± 0.006 | 11.68 ± 2.59 | 2.65 ± 0.01 | 0.13 ± 0.04 | 257.34 ± 3.44 | 436.38 ± 28.88 | 273.61 ± 2.98 |
| **PSMA in complex with N-terminal RA** | 0.22 ± 0.01 | 2.51 ± 0.007 | 17.42 ± 3.13 | 2.66 ± 0.01 | 0.13 ± 0.05 | 268.9 ± 3.44 | 514.35 ± 28.96 | 276.86 ± 3.94 |

PSMA, Prostate-specific membrane antigen; RA, recombinant albumin; RMSD, root mean square deviation; Rg, radius of gyration; ANHB, average number of hydrogen bonds; RMSF, root mean square deviation; SASA, solvent accessible surface area; ANC, average number of contacts.

The RMSD plot showed that the simulation had converged, and the simulation time was enough. The final structure obtained from step 5 was used for docking the PSMA domain to RA (step 6). The docking scores of the PSMA domain to the C-terminal and N-terminal of RA were -122.9 ± 9.5 and -132.9 ± 2.2, respectively. Then, the propensity of the PSMA domain to the N-terminal of RA was greater than the C-terminal of RA. Also, the Z-scores of these dockings were -1.9 and -1.3, respectively. Z-score specifies how many standard deviations from the average this cluster is located in terms of score (the more negative the better). The negative Z-score shows the top-ranked cluster (50).

Then, RA could bind to the extracellular domain of the PSMA protein on the surface of cancerous cells. To better investigate the interaction of the PSMA domain with RA, the MDS of the PSMA-RA complexes obtained from docking was performed (step 7). Figure 5 shows the backbone RMSD of PSMA in complex with the C-terminal and N-terminal of RA during 100 ns of MDS.

The backbone RMSD of the PSMA receptor domain decreased after binding to RA. The cause of this occurrence is probably the creation of hydrogen and hydrophobic bonds between the PSMA domain and RA that constrain PSMA atom displacement relative to its initial position. The other cause is probably the use of the final structure of the free PSMA receptor domain (after 100 ns MDS) as the starting structure for docking of PSMA to RA in PSMA-RA complexes simulation.

Also, the average of the backbone RMSD of RA in free form or when the PSMA receptor domain bound to its N-terminal or C-terminal was 1.15 ± 0.025 nm, 0.23 ± 0.01 nm, and 0.21 ± 0.01 nm, respectively. It means the displacement of RA atoms decreased after binding the PSMA receptor domain to it, and the PSMA domain could induce structural limitation in RA structure.

Table 3 shows the simulation parameters of the PSMA domain in complex with the C-terminal or N-terminal of RA during the last 30 ns of MDS. As revealed in Table 3, on average, about 17 or 11 hydrogen bonds (ANHB) were made during the last 30 ns of MDS between the PSMA receptor domain and the N-terminal or C-terminal of RA, respectively. In other words, the PSMA domain had a greater tendency to the N-terminal relative to the C-terminal of RA, this was compatible with Haddock scores. The average number of contacts (ANC) between the PSMA domain and RA was also compatible with these results. The Rg of the PSMA domain in complex with RA was more than the free-form RA, so binding RA induced partial structural changes in the PSMA receptor domain. The average SASA of the PSMA domain and RMSF of PSMA in complex with RA increased relative to the free PSMA domain. In other words, despite the expectation for a decrease of SASA of the PSMA receptor in complex,

binding RA to the PSMA receptor induced structural changes in the PSMA domain structure, increased the SASA of non-bonded parts, and decreased bonded parts of the PSMA domain, the whole SASA of the PSMA domain partially increased (Table 3).

The hydrogen and hydrophobic interactions of residues of the N-terminal and C-terminal of RA with the PSMA domain were calculated *via* module DIMPLOT of LigPlot software at the end of 100 ns of MDS in these complexes and are mentioned in Table 4. Table 4 also confirmed the proper interaction of the N-terminal and C-terminal of RA with the PSMA domain. Also, the interacting residues of the complex of the PSMA domain and the N-terminal or C-terminal of RA in the final structures were represented in Fig. 6.

The PCA analyses of the RA-PSMA complex showed that the first 2 eigenvalues for the free PSMA domain and the PSMA domain in complex with the N-terminal and C-terminal of RA were 1.22 and 0.48, 1.64 and 1.34, and 1.06 and 0.26, respectively. The plot of PC1 versus PC2 during the last 30 ns of MDS for Cα displacement in RA when the PSMA receptor bound to its C-terminal or N-terminal was represented in Fig. S2. The comparison of the plot of free RA with these results confirmed that binding the PSMA domain to the N-terminal or C-terminal of RA induced different structural changes in RA conformation.

In addition, the FEL of the free PSMA domain and PSMA in the complex with the C-terminal or N-terminal of RA (step 7) and RA in the complex with the PSMA domain were represented in Fig. 7. The wide basin blue areas in free and complex form showed that simulations converged and the PSMA domain acquired many stable and low-energy conformations during the last 30 ns of MDS. The difference between the free PSMA receptor domain and the bonded PSMA receptor showed that binding RA to the PSMA domain induced structural changes in PSMA and reduced wide blue stable conformations relative to free PSMA. The number of vertices increased, but the height decreased after binding to the N-terminal or C-terminal of RA. Then, the PSMA domain in complex with RA could change its conformation easily and pass over the free energy barriers. A similar event was seen in the FEL of RA in the complex with the PSAM domain. It revealed the extensive stable conformation area and conformation changes of RA when the C-terminal or N-terminal bound to the PSMA domain. The number of free energy barriers (red vertex) and the height of the free energy barrier in RA when the N-terminal had contact with the PSMA domain were higher relative to the C-terminal contact. In total, the difference in FEL plots between free and complex PSMA and RA confirmed the binding PSMA domain to RA.

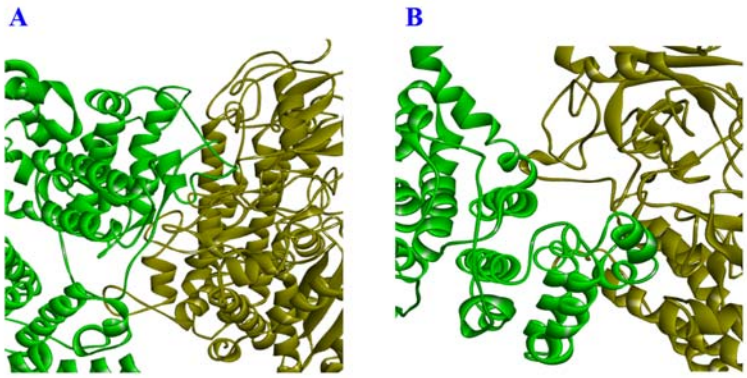


**Fig. 6**: 3D picture of complex prostate-specific membrane antigen receptor (brown) with the (A) N-terminal and (B) C-terminal of recombinant albumin (green).

**Table 4.** The number of residues of RA and PSMA domain that have contact with each other at the end of 100 ns of simulation in complexes.

| N-terminal contacts | | C-terminal contacts | |
|---|---|---|---|
| **Hydrogen bonds** | | | |
| **RA residue** | **PSMA residue** | **RA residue** | **PSMA residue** |
| Arg2 (THP) | Asp184 | His20 (THP) | Lys610 |
| Phe3 (THP) | Ser317 | Asp16 (THP) | Glu505, Ser503 |
| Arg10 (THP) | Pro504 | Glu393 (HSA) | Arg320 |
| Leu12 (THP) | Lys207 | Phe395 (HSA) | Arg190 |
| Ser15(THP) | Val208 | Glu396 (HSA) | Met192, Ser312, Ala313 |
| Ala16 (THP) | His 697 | Lys545 (HSA) | Asp184 |
| Ala19 (THP) | Asp184 | Asp550 (HSA) | Lys617 |
| Ala20 (THP) | Asp184 | Glu556 (HSA) | His618 |
| Lys21 (THP) | Arg190 | Lys557 (HSA) | Ser613 |
| Lys41 (HSA) | Pro504, Glu505 | | |
| Asp56 (HSA) | Asp316, Ser317 | | |
| Ala78 (HSA) | Ser507 | | |
| Arg114 (HSA) | Glu486 | | |
| Leu115 (HSA) | Glu486 | | |
| Thr133 (HSA) | Lys545 | | |
| Asn503 (HSA) | Glu489 | | |
| **Hydrophobic bonds** | | | |
| **THP** | **HSA** | **THP** | **HSA** |
| Gly1, Thr8, Gly9, Arg13, Ile14, Glu17, Ala18, Glu22 | Gln33, Cy34, Pro35, Phe36, Glu37, Asp38, Val40, Thr52, Thr76, Val77, Glu82, Thr83, Asn111, Leu112, Pro113, Glu119, Asp121, Met123, Ala126, Lys136, Lys137, Lys500, Glu505, Phe506, Gly508 Lys539, Asn540, Trp541, Glu542, Thr543, Phe546, Ser547, Gly548, Tyr549, Lys617, Lys623, Asn698, Tyr700, Tyr709, Phe713 | Lys6, Glu7, Ala8, Ala9, Lys11, Ala12, Trp13, Thr17, His19, Thr23 | Gln397, Gly399, Lys439, Ala553, Phe554, Glu189, Asp191, Pro315, Trp319, Pro504, Arg511, Thr538, Lys539, Asn540, Trp541, Lys545, Phe546, Tyr612, Met616, Pro619, Glu703, Tyr709 |

THP, Tumor-homing peptide residues; HSA; human serum albumin; RA, recombinant albumin; PSMA, prostate-specific membrane antigen.

***Frustration study***

Frustration is a valuable perception for the acquisition vision of the biological behaviour of proteins by analyzing how the energy is scattered in protein structures and how mutations or conformational changes shift the energetics. Two types of frustration can be considered: mutational frustration (which shows how beneficial the native residues are relative to other residues in that location) and configurational frustration (which indicates how suitable the native interactions between two residues are relative to other interactions between these residues that can form in other compact structures) (51). In this study, we calculated the configurational frustration index. The frustration index measured how agreeable a particular contact was relative to the set of all possible contacts in that location, normalized *via* the variance of that distribution. A contact was defined as minimally frustrated if it had a frustration index of 0.78 or higher; this means the majority of other amino acid pairs in that position would be undesirable. On the other hand, a contact was defined as highly frustrated if it had a local frustration index < -1, which means most other amino acid pairs at that location would be more favourable for folding than the native ones by more than one standard deviation of that distribution. If the native energy was between these limits, the contact was defined as neutral (51). The sites of high local frustration often show biologically important regions involved in binding or allostery and make clusters on the protein surface.

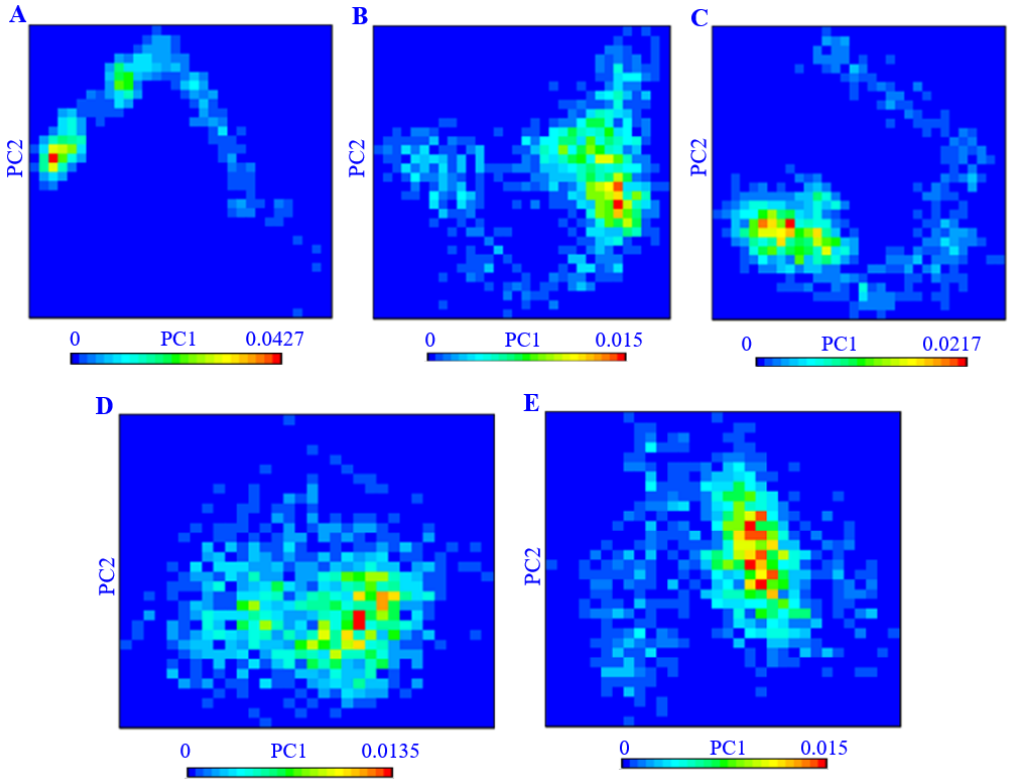


**Fig. 7.** Free energy landscape of free PSMA domain receptor and PSMA domain in complex with the N-terminal and C-terminal of RA and RA in complex with PSMA domain during the 30 ns of simulation. (A) Free PSMA domain; (B) PSMA domain in complex with C-terminal of RA; (C) PSMA domain in complex with N-terminal of RA; (D) RA in complex with PSMA domain (C-terminal); and (E) RA in complex with PSMA domain (N-terminal). PSMA, Prostate-specific membrane antigen; RA, recombinant albumin.

The configurational frustration index for the interacting pair of PSMA and RA in the complex was calculated *via* the frustratometer web server (http://frustratometer.qb.fcen.uba.ar) (52,53) in the final structure of the complex with RA with docetaxel, cabazitaxel, and doxorubicin, and also in PSMA/RA complexes. According to the server results, the number of highly frustrated pair residues of RA in contact with docetaxel, doxorubicin, and cabazitaxel was 301, 321, and 327, respectively, which had a reverse relationship with binding affinity order. In other words, the less highly frustrated pair residues in the complex (in this case, for docetaxel) probably lead to the more stable complex structure and more binding affinity of the drug to RA. Also, in complex PSMA-RA, only pairs K240/A149, P502/E60, E542/D144, and K699/S15 in the PSMA/RA N-terminal complex had high frustration contact, and 308 pairs had minimal or neutral frustration contact. In addition, pairs D184/D572, L188/Q420, D191/E419, M192/E419, P315/E416, P315/L417, P315/Q420, D316/E416, E505/D621, M616/K580, and K617/F577 in the PSMA/RA C-terminal complex had high frustration contact, and 181 pairs had minimal or neutral frustration contact. The smaller number of destabilizing residue pairs (with high configurational frustration contact) in the PSMA/RA N-terminal complex showed a more stable PSMA/RA N-terminal complex relative to the C-terminal complex after 100 ns MDS and then better interaction in the PSMA receptor with the N-terminal of RA. The distinct configurational contact maps of RA with drugs and with PSMA at the N-terminal and C-terminal of RA were represented in Fig. S4, and the different frustration patterns were circled.

## DISCUSSION

The anti-prostate cancer drugs such as docetaxel, cabazitaxel, and doxorubicin have hydrophobic properties, and transferring them into the blood has many problems. Therefore, finding drug carriers for them is a very important subject. The targeted delivery of anticancer drugs to cancerous cells is an important goal in drug delivery. It helps to drive anticancer drugs to the targeted cancerous cells and reduce the needed dose for use and side effects. Non-target consumption of drugs leads to the destruction of normal cells and drug delamination and metabolism by CYP3A subfamily enzymes in the liver (3). An interesting issue in prostate cancer is that these cells express the PSMA receptor on their cell surface. This receptor can be used for drug delivery and to improve the pharmacological profile of anti-prostate drugs by connecting tumor-homing peptides to albumin to direct albumin molecules to cancer cells (54). Albumin is a very abundant protein in the blood, and its task is the transfer of substrates such as fatty acids, bilirubin, and thyroxine in the blood (7,12,13,25). Then, this protein was chosen for drug delivery in some studies. In addition, it has the potential to promote half-life extension and targeted delivery of drugs (8). It has an affinity for anionic and hydrophobic compounds (13). Also, some therapeutic proteins had been specifically bound to albumin, and then their circulatory half-life was extended (7).

In this study, at first, doxorubicin, docetaxel, and cabazitaxel docked to native albumin, and the results showed that the order of binding affinity of drugs to native albumin was doxorubicin, docetaxel, and cabazitaxel, respectively, and then native albumin alone could be used for the transfer of these drugs. Experimental studies have shown that docetaxel and doxorubicin are extensively bound to albumin (3,13,18-24). As well as the binding of several important classes of oncology drugs to native albumin was indicated by Spada *et al*. (8). The present results were compatible with other investigations. Among these drugs, doxorubicin had better binding energy to albumin, probably due to its smaller volume. The VDW energies of the best pose were more negative than the electrostatic energies. The perusal of binding residues indicated that the binding site of all drugs was a hydrophobic pocket. This was expected because all drugs had heterocyclic structures.

Two tumor-homing peptides alongside a rigid linker were connected to the N-terminal and C-terminal of native albumin and made an RA for drug delivery. At first, the RA was simulated for 100 ns in the presence of water

and ions to reach a stable structure. Then, these drugs were docked to simulated RA and showed that the trend of binding affinity in docking unmodified albumin and modified albumin was the same, but interestingly, modified albumin had more affinity than native albumin. Then, the tumor-homing peptides in RA tails probably induce proper structural changes in the binding sites of RA that lead to better interaction of drugs with it.

The complexes of drugs with RA were simulated for 100 ns, and the results showed that they remained joint to RA during the 100 ns MDS. The final picture of complexes showed that both cabazitaxel and docetaxel (with similar structures) bound to site IB, and doxorubicin bound to site IIA of RA. Site IB had the capacity for large heterocyclic compounds. These results were compatible with previous results that indicated that sites IB and IIA were more abundant sites for ligand binding in albumin relative to other sites (13).

At first, the free RA was simulated and its structure reached equilibrium and became stable; then this structure was used for docking and MDS; therefore, the backbone RMSD of RA at complexes was lower than free RA (Fig. 1), and the backbone atoms did not change their position relative to the starting position significantly. Also, the creation of new interactions between drugs and RA in complexes could lead to a decrease in RMSD or a constant RMSD of RA in complexes relative to free form. Indeed, the drugs stabilized the RA structure. No change in Rg and RMSF of RA in complexes relative to free RA was seen (Table 1), which means no large conformational changes upon ligand binding in drug-bound forms compared to free RA. In other words, drug binding did not change RA compactness (tertiary structure) or total flexibility (RMSF) of RA or induce only marginal changes. Also, a trivial increase in SASA in the ligand-bond form of RA relative to the free form was seen (Table 1).

Sasidharan *et al.* showed that the ligand-bound forms of the estrogen-related gamma receptor had similar or the same Rg, RMSF, and RMSD and increased SASA relative to the apo form of the protein, and the apo form was very stable in binding (55). These results were similar to the current work and could support the results. Also, trivial decreases in the α-helix content of RA upon drug binding in this work were similar to the results of Karami *et al*. showed that binding of salicylic acid with HSA decreased the α-helix content of HSA (56).

However, in drug binding, some protein atoms made hydrogen bonds with drugs instead of protein atoms, and then the number of hydrogen bonds RA with itself reduced (Table 1).

The MM/PBSA binding free energy results during 100 ns MDS revealed that docetaxel, doxorubicin, and cabazitaxel, respectively, had a binding affinity to RA. The simulation results were almost similar to the docking results.

Proteins achieve their function by collective atomic motions; therefore, they can be used to describe important functions, such as folding, stability, and ligand binding (53). PCA, in this study, showed the conformational motion of free and complex RA.

Results showed that bond forms of RA occupied more conformational space along PC1 and PC2 as compared to the free form (Fig. S2A-D). The changes in conformational space possibly arose due to differences in their collective residual motion along both PC1 and PC2. The main directions of the Cα movements and also the number of high-energy regions in the FEL of the complexes compared to free RA were changed upon drug binding (Fig. 2). Because of the trivial height of the free energy barrier and the small number of them in the FEL of RA in complexes relative to unbound RA (free RA), it seems that conformational transition due to a population redistribution between them was easy, and these complexes had appropriate kinetic release behaviour and fast drug release. The changes in the PC1-PC2 plot due to ligand binding were reported by Deshpande *et al*., which were comparable to the current results (57).

The drug residence time was calculated and reported using the RAMD method. The residence time of compounds is a major factor in the extent of their pharmacological effects. The drugs were released from RA at the picosecond time scale; docetaxel had a longer retention time than other drugs and a slower release than other drugs; cabazitaxel had a

shorter retention time and was released easily. However, for the fast release of anticancer drugs, cabazitaxel can be used. Vice versa, docetaxel can be used in combination with RA.

Voss *et al.* showed a sharp relationship between ligand affinity and residence time in some macrocyclic $G\alpha_q$ protein inhibitors (58). This study showed a linear relationship between residence time and binding free energy of 3 drugs with RA ($R^2 = 0.4$). The low coefficient of determination ($R^2$) was probably due to the low number of points (3 drugs).

The small energy barrier in FEL of complexes and similar FEL of complexes means easy conformational change, which was compatible with a low residence time of drugs.

On the other hand, the extracellular domain of the PSMA protein structure was docked to the N-terminal and C-terminal of RA separately, and it was shown that RA could bind to them. The MDS of RA-PSMA complexes supported these results. Also, PCA analysis confirmed proper binding of the PSMA receptor to the N-terminal and C-terminal of RA.

The decrease in RMSD of PSMA after binding to RA was probably due to limiting interactions in the complex PSMA-RA that prevented displacement of PSMA atoms. A trivial increase in Rg and total SASA values of PSMA in complexes relative to free PSMA (Table 3) represented a little change in the structural conformation of the PSMA after complex formation (at most 1% in Rg and 5% in total SASA). Visual investigation of complexes showed that PSMA had a relatively small contact surface with RA (C-terminal and N-terminal tails), and then its surface did not change significantly relative to free PSMA. Also, an increase in SASA in non-contact surface parts of PSMA probably neutralized the SASA decrease in the contact surface section of PSMA, and the total SASA of PSMA was not changed or increased, insignificantly.

According to PCA analysis of the complex with the N-terminal and C-terminal of RA, it revealed that complex formation did not change large conformational motions of the PSMA domain or RA proteins because the eigenvalues for the free PSMA domain and PSMA in complexes were similar and near each other.

Frustration analysis disclosed the location of frustration in protein structure and indicated how mutations or conformational changes shifted the frustration state. The lower number of destabilizing residue pairs in the contact surface of the complex docetaxel relative to other drugs and also in the PSMA/RA N-terminal complex relative to the C-terminal complex showed that these complexes were more stable than others.

## CONCLUSION

This study revealed that a newly engineered albumin has suitable thermodynamics and kinetics characterization for binding to docetaxel, doxorubicin, cabazitaxel, and PSMA receptor. Therefore, this RA can be used as a human albumin-based therapeutic carrier for prostate cancer treatment. This new RA can enhance the distribution and bioavailability of some anticancer drugs. RA should be cloned and made, and its ability to bind and release the drugs should be tested experimentally. This work offered the first real hope of maximizing the anticancer drug efficiency and tolerability for targeted drug delivery and reducing the side effects of anticancer drugs due to binding to non-cancer cells. It hopes this work sheds light on a better cure for cancer disease.

There are some suggestions for future studies. The half-life extension of RA because of the covalent binding of tumor-homing peptides to it should be tested theoretically or experimentally in future work. Also, the probable structural changes due to the acidic environment of cancerous tissue (59) in the structure of RA and its effect on drug release can be investigated by MDS of RA in acidic conditions of these drugs in future works. In addition, because albumin molecules have some receptors in the body such as gp18, gp30, gp60, cubulin, megalin, and the neonatal Fc receptor (FcRn) (7), it is suggested some point mutation designs in this RA in future studies for the prohibition of binding it to other normal cells (for example inhibition of albumin/FcRn interaction) and make it more specific for cancerous cells. On the other hand, the influence of the linker length that connects peptides to albumin in RA on the

binding of RA to the PSMA domain and the release rate of drugs can be tested in future work. Finally, to decrease the cost of production of RA gene fusion, it is suggested that only sites IB and IIA of albumin are made for the construction of RA in the drug delivery of these drugs.

***Acknowledgment***

The Research Council of Shahrekord University financially supported the study.

***Conflict of interest statement***

All authors declared no conflict of interest in this study.

***Authors' contributions***

All authors contributed to the work described in this paper equally. All authors take responsibility for the integrity of the work as a whole from inception to published article and are designated as 'guarantor' and take the responsibility for it. All authors read and approved the final version of the manuscript.

## REFERENCES

1. Rawla P. Epidemiology of prostate cancer. World J Oncol. 2019;10(2):63-89. DOI: 10.14740/wjon1191.
2. Paal K, Shkarupin A, Beckford L. Paclitaxel binding to human serum albumin-automated docking studies. Bioorg Med Chem. 2007;15(3):1323-1329. DOI: 10.1016/j. bmc.2006.11.012.
3. Carbonetti G, Converso C, Clement T, Wang C, Trotman LC, Ojima I, *et al*. Docetaxel/cabazitaxel and fatty acid binding protein 5 inhibitors produce synergistic inhibition of prostate cancer growth. Prostate. 2020;80(1):88-98. DOI: 10.1002/pros.23921.
4. Sousa-Pimenta M, Estevinho LM, Szopa A, Basit M, Khan K, Armaghan M, *et al*. Chemotherapeutic properties and side-effects associated with the clinical practice of terpene alkaloids: paclitaxel, docetaxel, and cabazitaxel. Front Pharmacol. 2023;14:1157306,1-14. DOI: 10.3389/fphar.2023.1157306.
5. Vigevani A, Williamson MJ. Doxorubicin. In: Klaus Florey, Editor. Analytical profiles of drug substances. Vol 9. New York: Academic Press; 1981. pp. 245-274.
6. Khoeeniha MK, Esfandyari-Manesh M, Behrouz H, Amini M, Shiri Varnamkhasti B, Atyabi F., *et al*. Targeted delivery of cabazitaxel by conjugation to albumin-PEG-folate nanoparticles using a cysteine-acrylate linker and simple synthesis conditions. Curr Drug Deliv. 2017;14(8):1120-1129. DOI: 10.2174/1567201814666161122150302.
7. Sleep D, Cameron J, Evans LR. Albumin as a versatile platform for drug half-life extension. Biochym Biophys Acta. 2013;1830(12):5526-5534. DOI: 10.1016/j.bbagen.2013.04.023.
8. Spada A, Emami J, Tuszynski JA, Lavasanifar A. The uniqueness of albumin as a carrier in nanodrug delivery. Mol Pharmaceutics. 2021;18(5):1862-1894. DOI: 10.1021/acs. molpharmaceut.1c00046.
9. Nezir AE, Khalily MP, Gulyuz S, Ozcubukcu S, Küçükgüzel SG, Yilmaz O, *et al*. Synthesis and evaluation of tumor-homing peptides for targeting prostate cancer. Amino Acids. 2021;53(5):645-652. DOI: 10.1007/s00726-021-02971-3.
10. Ghosh A, Heston WDW. Tumor target prostate specific membrane antigen (PSMA) and its regulation in prostate cancer. J Cell Biochem. 2004;91(3):528-539. DOI: 10.1002/jcb.10661.
11. Aggarwal S, Singh P, Topaloglu O, Isaacs JT, Denmeade SR. A dimeric peptide that binds selectively to prostate-specific membrane antigen and inhibits its enzymatic activity. Cancer Res. 2006;66(18):9171-9177. DOI: 10.1158/0008-5472.CAN-06-1520.
12. Van de Sande L, Cosyns S, Willaert W, Ceelen W. Albumin-based cancer therapeutics for intraperitoneal drug delivery: a review. Drug Deliv. 2020;27(1):40-53. DOI: 10.1080/ 10717544.2019.1704945.
13. Carter DC. Crystallographic survey of albumin drug interaction and preliminary applications in cancer chemotherapy. In: Abraham DJ, Rotella DP, Editors. Burger's medicinal chemistry, drug discovery, and development. 7th ed. Hoboken: John Wiley & Sons Inc; 2010. pp: 437-468. DOI: 10.1002/0471266949.bmc166.
14. Rahimizadeh P, Yang S, Lim SI. Albumin: an emerging opportunity in drug delivery. Biotechnol Bioprocess Eng. 2020;25:985-995. DOI: 10.1007/s12257-019-0512-9.
15. Challapa-Mamani MR, Tomás-Alvarado E, Espinoza-Baigorria A, León-Figueroa DA, Sah R, Rodriguez-Morales AJ, *et al*. Molecular docking and molecular dynamics simulations in related to *Leishmania donovani*: an update and literature review. Trop Med Infect Dis. 2023;8(10):457,1-13. DOI: 10.3390/tropicalmed8100457.
16. Elsadek B, Kratz F. Impact of albumin on drug delivery-new applications on the horizon. J Control Release. 2012;157(1):4-28. DOI: 10.1016/j.jconrel.2011.09.069.
17. Kratz F. Albumin as a drug carrier: design of prodrugs, drug conjugates and nanoparticles. J Control Release. 2008;132(3):171-183. DOI: 10.1016/j.jconrel.2008.05.010.
18. Qu N, Sun Y, Li Y, Hao F, Qiu P, Teng L, *et al*. Docetaxel-loaded human serum albumin (HSA) nanoparticles: synthesis, characterization, and evaluation. Biomed Eng Online. 2019;18(1):11,1-14.

DOI: 10.1186/s12938-019-0624-7.
19. Su Z, Zhao J, Zhao X, Xie J, Li M, Zhao D. Preclinical evaluation of albumin-bound docetaxel nanoparticles as potential anti-cancer products. Int J Pharm. 2023;635:122711. DIO: 10.1016/j.ijpharm.2023.122711.
20. Urien S, Barré J, Morin C, Paccaly A, Montay G, Tillement JP. Docetaxel serum protein binding with high affinity to alpha1-acid glycoprotein. Invest New Drugs. 1996;14(2):147-151. DOI: 10.1007/BF00210785.
21. Qi WW, Yu HY, Guo H, Lou J, Wang ZM, Liu P, *et al*. Doxorubicin-loaded glycyrrhetinic acid modified recombinant human serum albumin nanoparticles for targeting liver tumor chemotherapy. Mol Pharmaceutics. 2015;12(3):675-683. DOI: 10.1021/mp500394v.
22. Di Stefano G, Fiume L, Baglioni M, Bolondi L, Chieco P, Kratz F, *et al*. Efficacy of doxorubicin coupled to lactosaminated albumin on rat hepatocellular carcinomas evaluated by ultrasound imaging. Dig Liver Dis. 2008;40(4):278-284. DOI: 10.1016/j.dld.2007.10.008.
23. Maltas E, Gubbuk IH, Yildiz S. Development of doxorubicin loading platform-based albumin-sporopollenin as drug carrier. Biochem Biophys Rep. 2016;7:201-205. DOI: 10.1016/j.bbrep. 2016.06.012.
24. Agudelo D, Bourassa P, Bruneau J, Bérubé, G, Asselin É, Tajmir-Riahi HA. Probing the binding sites of antibiotic drugs doxorubicin and N-(trifluoroacetyl) doxorubicin with human and bovine serum albumins. PLoS One. 2012;7(8):e43814,1-13. DOI: 10.1371/journal.pone.0043814.
25. Larsen MT, Kuhlmann M, Hvam ML, Howard KA. Albumin-based drug delivery: harnessing nature to cure disease. Mol Cell Ther. 2016;4(3):1-12. DOI: 10.1186/s40591-016-0048-8.
26. Wacker M. Nanocarrier for intravenous injection-long hard road to market. Int J Pharm. 2013:457(1):50-62. DOI: 10.1016/j.ijpharm.2013.08.079.
27. Rezaei L, Safavi MS, Shojaosadati SB. Protein nanocarriers for targeted drug delivery. In: Mohapatra SS, Ranjan S, Dasgupta N, Mishra RK, Thomas S, Editors. Characterization and biology of nanomaterials for drug delivery: nanoscience and nanotechnology in drug delivery. Amsterdam: Elsevier Science Publishing Co. Inc. 2018. DOI: 10.1016/B978-0-12-814031-4.00008-8.
28. Barkhordari A, Mahnam K, Mirmohammad-Sadeghi H. Designing a new bispecific tandem single-chain variable fragment antibody against tumor necrosis factor-α and interleukin-23 using *in silico* studies for the treatment of rheumatoid arthritis. J Mol Model. 2020;26(9):225,1-11. DOI: 10.1007/s00894-020-04510-5.
29. Mohammadian H, Mahnam K, Mirmohammad Sadeghi H, Ganjalikhany MR, Akbari V. Rational design of a new mutant of tobacco etch virus protease in order to increase the *in vitro* solubility. Res Pharm Sci. 2020;15(2):164-173. DOI: 10.4103/1735-5362.273816.
30. Abraham MJ, Murtola T, Schulz R, Páll S, Smith JC, Hess B, *et al*. GROMACS: high performance molecular simulations through multi-level parallelism from laptops to supercomputers. SoftwareX. 2015;1(2):19-25. DOI: 10.1016/j.softx.2015.06.001.
31. Morris GM, Goodsell DS, Halliday RS, Huey R, Hart WE, Belew RK, *et al*. Automated docking using a Lamarckian genetic algorithm and an empirical binding free energy function. J Comput Chem. 1998;19:1639-1662. DOI: 10.1002/(SICI)1096-987X(19981115)19:14<1639::AID-JCC10>3.0.CO;2-B.
32. Santos-Martins D, Eberhardt J, Bianco G, Solis-Vasquez L, Ambrosio FA, Koch A, *et al*. D3R Grand Challenge 4: prospective pose prediction of BACE1 ligands with AutoDock-GPU. J Comput Aided Mol Des. 2019;33(12):1071-1081. DOI: 10.1007/s10822-019-00241-9.
33. Chen X, Zaro J, Shen WC. Fusion protein linkers: property, design, and functionality. Adv Drug Deliv Rev. 2013;65(10):1357-1369. DOI: 10.1016/j.addr.2012.09.039.
34. Arai R, Ueda H, Kitayama A, Kamiya N, Nagamune T. Design of the linkers which effectively separate domains of a bifunctional fusion protein. Protein Eng. 2001;14(8):529-532. DOI: 10.1093/protein/14.8.529.
35. Amet N, Lee HF, Shen WC. Insertion of the designed helical linker led to increased expression of tf-based fusion proteins. Pharm Res. 2009;26(3): 523-528. DOI: 10.1007/s11095-008-9767-0.
36. Bai Y, Shen WC. Improving the oral efficacy of recombinant granulocyte colony-stimulating factor and transferrin fusion protein by spacer optimization. Pharm Res. 2006;23:2116-2121. DOI: 10.1007/s11095-006-9059-5.
37. Drozdetskiy A, Cole C, Procter J, Barton GJ. JPred4: a protein secondary structure prediction server. Nucleic Acids Res. 2015;43(W1):W389-W394. DOI: 10.1093/nar/gkv332.
38. Mahnam K, Rajaee SM. A theoretical survey to find potential natural compound for inhibition of binding the RBD domain to ACE2 receptor based on plant antivirals. J Biomol Struct Dyn. 2023;41(23):14540-14565. DOI: 10.1080/07391102. 2023.2183033.
39. Kumari R, Kumar R, Open Source Drug Discovery Consortium, Lynn A. g_mmpbsa, a GROMACS tool for high-throughput MM-PBSA calculations. J Chem Inf Model. 2014;54(7):1951-1962. DOI: 10.1021/ci500020m.
40. Dominguez C, Boelens R, Bonvin AMJJ. HADDOCK: a protein-protein docking approach based on biochemical or biophysical information. J Am Chem Soc. 2003;125(7):1731-1737. DOI: 10.1021/ja026939x.
41. Kokh DB, Amaral M, Bomke J, Grädler U, Musil D, Buchstaller HP, *et al*. Estimation of drug-target residence times by τ-random acceleration molecular

dynamics simulations. J Chem Theory Comput. 2018;14(7):1549-9618.
DOI: 10.1021/acs.jctc.8b00230.
42. Lüdemann SK, Lounnas V, Wade RC. How do substrates enter and products exit the buried active site of cytochrome P450cam? 2. steered molecular dynamics and adiabatic mapping of substrate pathways. J Mol Biol. 2000;303(5):813-830.
DOI: 10.1006/jmbi.2000.4155.
43. Duarte JM, Sathyapriya R, Stehr H. Filippis I, Lappe M. Optimal contact definition for reconstruction of Contact Maps. BMC Bioinformatics. 2010;11(283):7761,1-10.
DOI: 10.1186/1471-2105-11-283.
44. Sang P, Du X, Yang LQ, Meng ZH, Liu SQ. Molecular motions and free-energy landscape of serine proteinase K in relation to its cold-adaptation: a comparative molecular dynamics simulation study and the underlying mechanisms. RSC Adv. 2017;7(46):28580-28590.
DOI: 10.1039/c6ra23230b.
45. Amadei A, Linssen ABM, Berendsen HJC. Essential dynamics of proteins. Proteins. 1993;17(4):412-425.
DOI: 10.1002/prot.340170408.
46. Maisuradze GG, Liwo A, Scheraga HA. How adequate are one- and two-dimensional free energy landscapes for protein folding dynamics? Phys Rev Lett. 2009;102:238102,1-8.
DOI: 10.1103/PhysRevLett.102.238102.
47. Bai F, Xu Y, Chen J, Liu Q, Gu J, Wang X, *et al*. Free energy landscape for the binding process of Huperzine A to acetylcholinesterase. Proc Natl Acad Sci. 2013;110(11):4273-4278.
DOI: 10.1073/pnas.1301814110.
48. Wallace AC, Laskowski RA, Thornton JM. LIGPLOT: a program to generate schematic diagrams of protein-ligand interactions. Protein Eng. 1995;8(2):127-134.
DOI:10.1093/protein/ 8.2.127.
49. Lozano-Aguilera ED, Estudillo-Martínez MD, Castillo-Gutiérrez S. A proposal for plotting positions in probability plots. J Appl Stat. 2014;41(1):118-126.
DOI: 10.1080/02664763.2013.831814.
50. Mohammadi pour P, Mahnam K, Taherzadeh M, Ahangarzadeh S, Alibakhshi A, Mohammadi E. The effect of mutation on neurotoxicity reduction of new chimeric reteplase, a computational study. Res Pharm Sci. 2023;18(4):404-412.
DOI: 10.4103/1735-5362.378087.
51. Jenik M, Parra RG, Leandro GR, Radusky LG, Turjanski A, Peter G, *et al*. Protein frustratometer: a tool to localize energetic frustration in protein molecules. Nucleic Acids Res. 2012;40(W1):W348-W351.
DOI: 10.1093/nar/gks447.
52. Parra RG, Schafer NP, Radusky LG, Tsai MY, Guzovsky AB, Wolynes PG, *et al*. Protein Frustratometer 2: a tool to localize energetic frustration in protein molecules, now with electrostatics. Nucleic Acids Res. 2016;44(W1):W356-W360.
DOI: 10.1093/nar/gkw304.
53. Amir M, Ahmad S, Ahamad S, Kumar V, Mohammad T, Dohare R, *et al*. Impact of Gln94Glu mutation on the structure and function of protection of telomere 1, a cause of cutaneous familial melanoma. J Biomol Struct Dyn. 2020;38(5):1514-1524.
DOI:10.1080/07391102.2019.1610500.
54. Pal S, Reshma G B, Mohny FP, Choudhury SG, Karmakar A, Gupta S, *et al*. Albumin nanoparticles surface decorated with a tumor-homing peptide help in selective killing of triple-negative breast cancer cells. ACS Appl Mater Interfaces. 2023;15(40):46721-46737.
DOI: 10.1021/acsami.3c11561.
55. Sasidharan S, Radhakrishnan K, Lee JY, Saudagar P, Gosu V, Shin D. Molecular dynamics ERRγ ligand binding domain with agonist and inverse agonist. PLoS One.2023;18(4):e0283364,1-18.
DOI: 10.1371/journal.pone.0283364.
56. Karami L, Tazikeh-Lemeskib E, Saboury AA. Molecular dynamics simulation and free energy studies on the interaction of salicylic acid with human serum albumin (HSA). Phys Chem Res. 2017;5(3):483-496.
DOI: 10.22036/pcr.2017.63757.1315.
57. Deshpande SH, Bagewadi ZK, Khan TMY, Mahnashi MH, Shaikh IA, Alshehery S, *et al*. Exploring the potential of phytocompounds for targeting epigenetic mechanisms in rheumatoid arthritis: an *in silico* study using similarity indexing. Molecules. 2023;28:2430,1-13.
DOI: 10.3390/molecules28062430.
58. Voss JH, Crüsemann M, Bartling CRO, Kehraus S, Inoue A, Gabriele M, *et al*. Structure-affinity and structure-residence time relationships of macrocyclic Gαq protein inhibitors. iScience. 2023;26(4):106492,1-19.
DOI: 10.1016/j.isci.2023.106492.
59. Tafech A, Stéphanou A. On the importance of acidity in cancer cells and therapy. Biology. 2024;13(4):225,1-25.
DOI: 10.3390/biology13040225.